

Supplementary Information

Novel thermally self-crosslinkable diaryluorene-based copolymers for efficient and stable blue light-emitting diodes

Alei Liu,^{a,#} Zhe Liu,^{ab,#} Hong Lin,^c Wenwei Tang,^a Zesen Lin,^a Weina Zhang,^a

Zhengjian Qi,^b Xiaofei Gu,^b Yueqi Mo,^{*,c} Lintao Hou^{*,a}

^a *Guangdong Provincial Key Laboratory of Optical Fiber Sensing and Communications, Guangzhou Key*

Laboratory of Vacuum Coating Technologies and New Energy Materials, Guangdong Provincial Engineering

Technology Research Center of Vacuum Coating Technologies and New Energy Materials, Siyuan Laboratory,

Department of Physics, Jinan University, Guangzhou 510632, PR China. Email: thlt@jnu.edu.cn

^b *Jiangsu Province Hi-Tech Key Laboratory for Biomedical Research, School of College of Chemistry and*

Chemical Engineering, Southeast University, Nanjing 211189, PR China

^c *Key Laboratory of Special Functional Materials, South China University of Technology, Guangzhou 510640, PR*

China. Email: pomoy@scut.edu.cn

[#] *These authors contributed to the work equally*

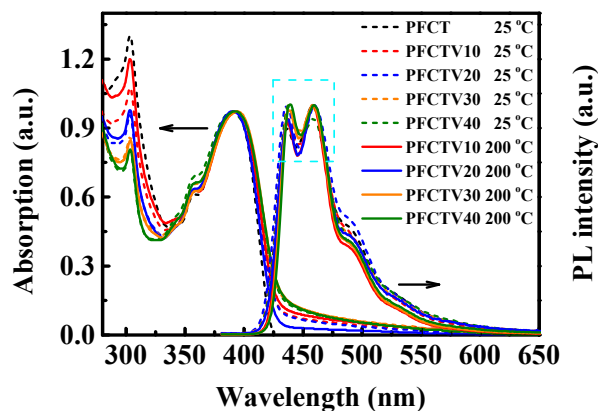


Fig. S1 UV-vis absorption and PL spectra of PFCT and PFCTV10–40 films.

Table S1. Optical properties and energy levels of PFCT and PFCTV10–40 with and without thermal crosslinking.

Polymers	$\lambda_{Abs, max}^a$	$\lambda_{Abs, max}^b$	$\lambda_{PL, max}^a$	$\lambda_{PL, max}^b$	E_g^a/E_g^b	E_{ox}	E_{HOMO}^a/E_{HOMO}^b	E_{LUMO}^a/E_{LUMO}^b
	(nm)	(nm)	(nm)	(nm)	(eV)	(eV)	E_{HOMO}^c	E_{LUMO}^c
PFCT	303.5	303.5	435	435	2.98/2.98	0.99	-5.39/-5.81/-	-2.41/-2.83/-
	391.0	391.0	457	457				
PFCTV10	303.5	303.5	436	436	2.96/2.96	0.97	-5.37/-5.77/-5.75	-2.41/-2.81/-2.79
	391.5	391.5	458	457				
PFCTV20	303.5	303.5	436	436	2.95/2.96	0.95	-5.35/-5.78/-5.69	-2.40/-2.83/-2.73
	391.5	390.5	459	457				
PFCTV30	303.5	303.5	436	436	2.93/2.94	0.94	-5.34/-5.79/-5.77	-2.41/-2.86/-2.83
	391.5	391.0	459	457				
PFCTV40	303.5	303.5	439	438	2.93/2.94	0.96	-5.36/-5.83/-5.81	-2.43/-2.90/-2.87
	391.5	390.0	459	458				

$\lambda_{Abs, max}^a$, $\lambda_{PL, max}^a$, $\lambda_{Abs, max}^b$ and $\lambda_{PL, max}^b$ are the main absorption and PL peaks of the films without/with annealing at 200 °C, respectively;

E_g^a and E_g^b are the optical band gaps determined by the cut off of absorption spectra of the films without/with annealing at 200 °C, respectively;

E_{HOMO}^a is calculated from the oxidation potentials E_{ox} from the *CV* curves with the equation of $E_{HOMO}^a = -(E_{ox} + 4.4)$ eV and $E_{LUMO}^a = E_{HOMO}^a + E_g^a$;

E_{HOMO}^b and E_{HOMO}^c are calculated from secondary electrons cut-off edge and valence-band maximum of UPS of the un-crosslinked and crosslinked films, respectively;

$E_{LUMO}^b = E_{HOMO}^b + E_g^b$ and $E_{LUMO}^c = E_{HOMO}^c + E_g^b$.

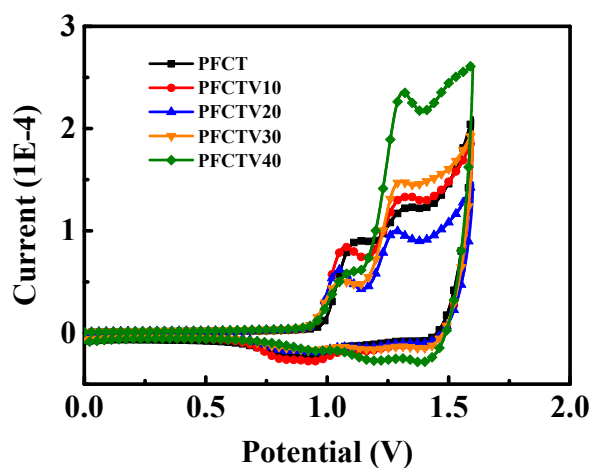


Fig. S2 *CV* characteristics of PFCT and PFCTV10–40 polymers.

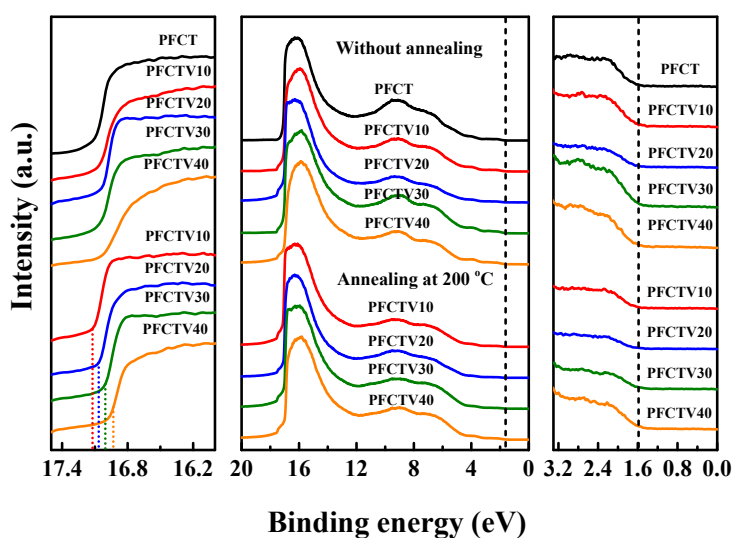


Fig. S3 UPS spectra of PFCT and PFCTV10–40 films.

Table S2. Detailed parameters of PFCT and PFCTV20 devices at the current density of around 35 mA/cm².

Device	Condition	Voltage (V)	J (mA/cm ²)	L (cd/m ²)	LE (cd/A)	EQE (%)
PFCT	25 °C	6	38.11	959.61	2.52	3.15
PFCTV20	25 °C	7.2	30.64	292.51	0.95	1.19
PFCTV20	200 °C-10min	5.2	38.15	1309.95	3.43	4.29

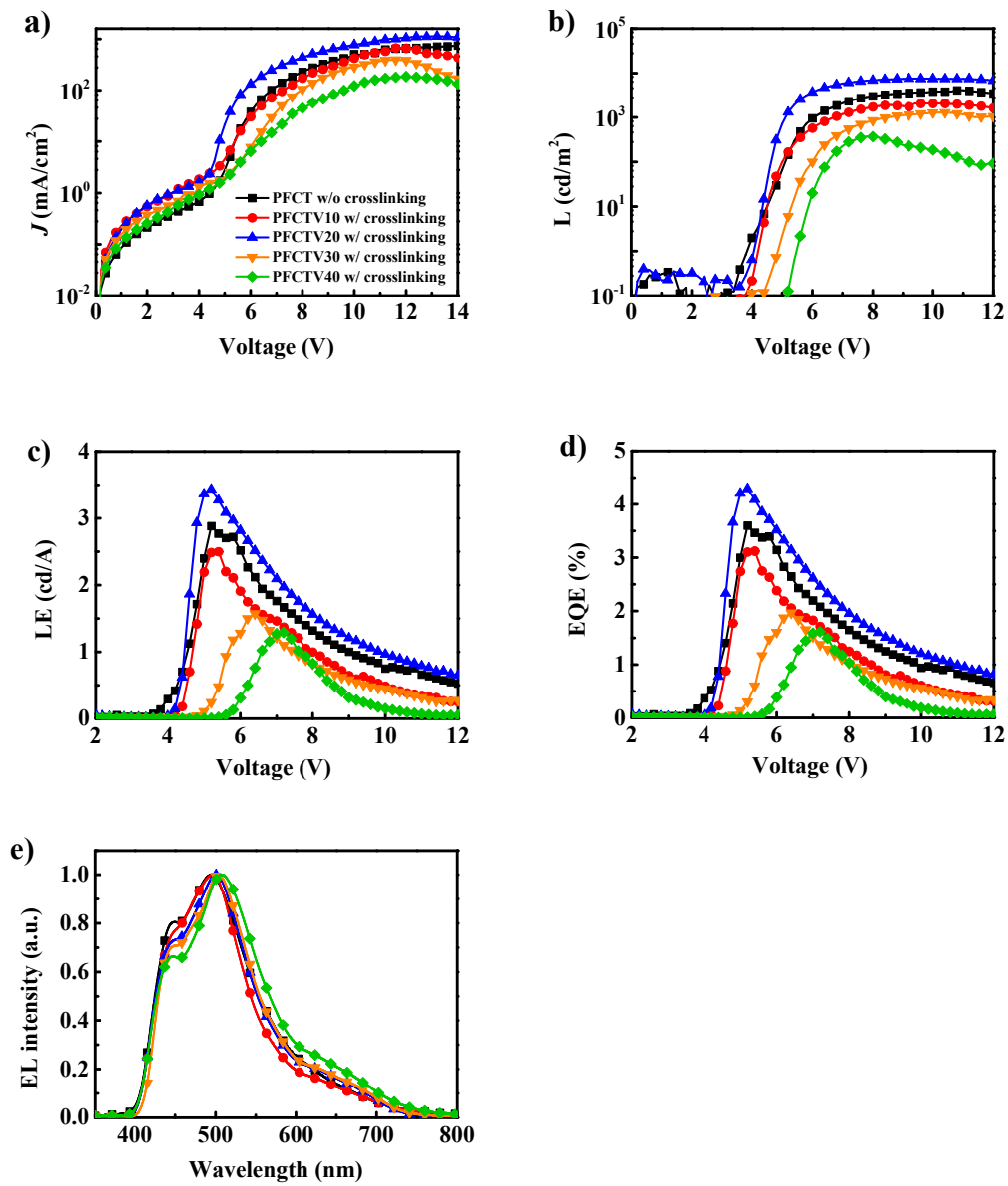


Fig. S4 J - V , L - V , LE - V , EQE - V characteristics and EL spectra of PFCT and PFCTV10–40 devices with thermal crosslinking at 200 °C.

Table S3. Detailed parameters of the PFCTV10–40 devices at the maximum LE and EQE under different crosslinking temperatures.

Device	T (°C)	V_{on} (V)	<i>Voltage</i> (V)	J (mA/cm ²)	L (cd/m ²)	LE (cd/A)	EQE (%)
PFCT	25	3.9	5.2	5.05	145.7	2.88	3.60
PFCTV10	25	4.9	6.8	6.76	86.5	1.28	1.60
	150	4.8	6.4	22.20	369.2	1.66	2.08
	200	4.3	5.4	10.31	257.7	2.50	3.12
	230	4.8	6	34.02	606.1	1.78	2.23
PFCTV20	25	5.4	6.2	2.58	56.2	2.17	2.72
	150	5.0	6.2	8.03	187.5	2.33	2.92
	200	4.3	5.2	38.15	1309.9	3.43	4.29
	230	4.6	6.8	144.55	2321.8	1.61	2.01
PFCTV30	25	5.6	8	31.70	324.4	1.02	1.28
	150	5.3	7.2	10.23	139.1	1.36	1.70
	200	4.9	6.4	15.45	243.1	1.57	1.97
	230	5.1	7	19.62	204.8	1.04	1.30
PFCTV40	25	5.7	9.4	879.31	3514.1	0.93	1.17
	150	5.5	7.2	21.93	282.9	1.29	1.61
	200	5.6	8	89.33	1010.8	1.13	1.41

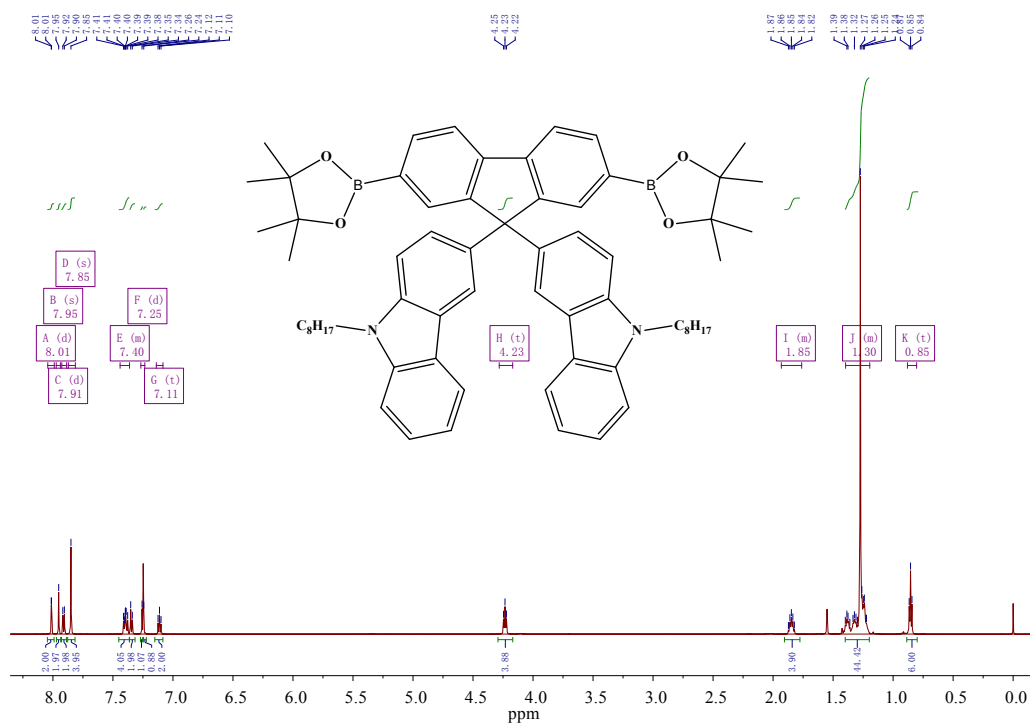


Fig. S5 1H -NMR of M1.

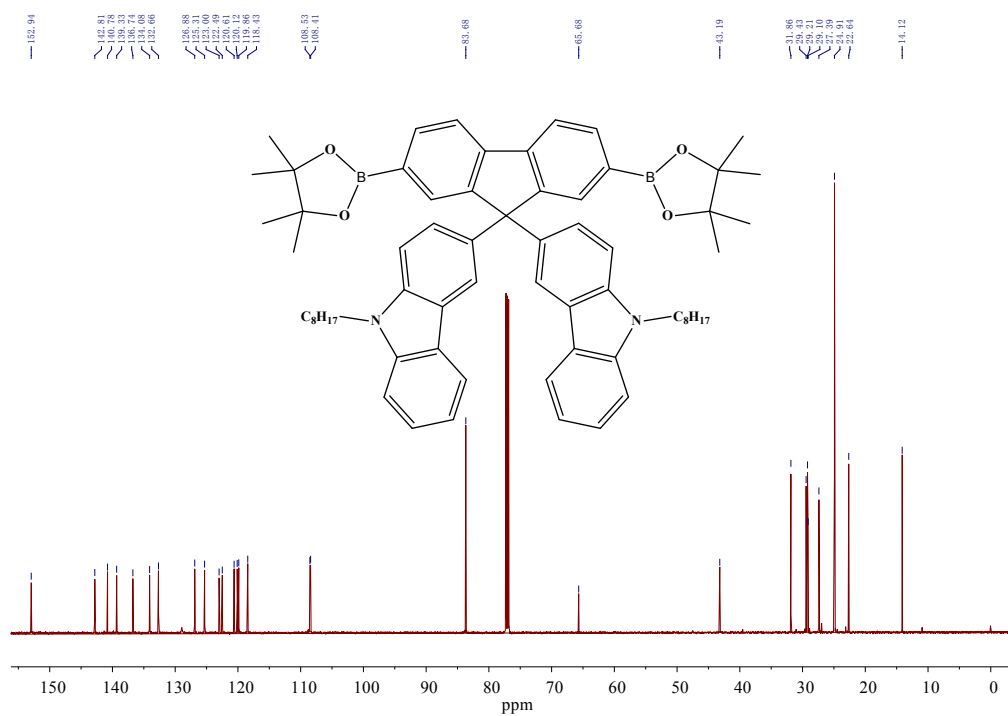


Fig. S6 ^{13}C -NMR of M1.

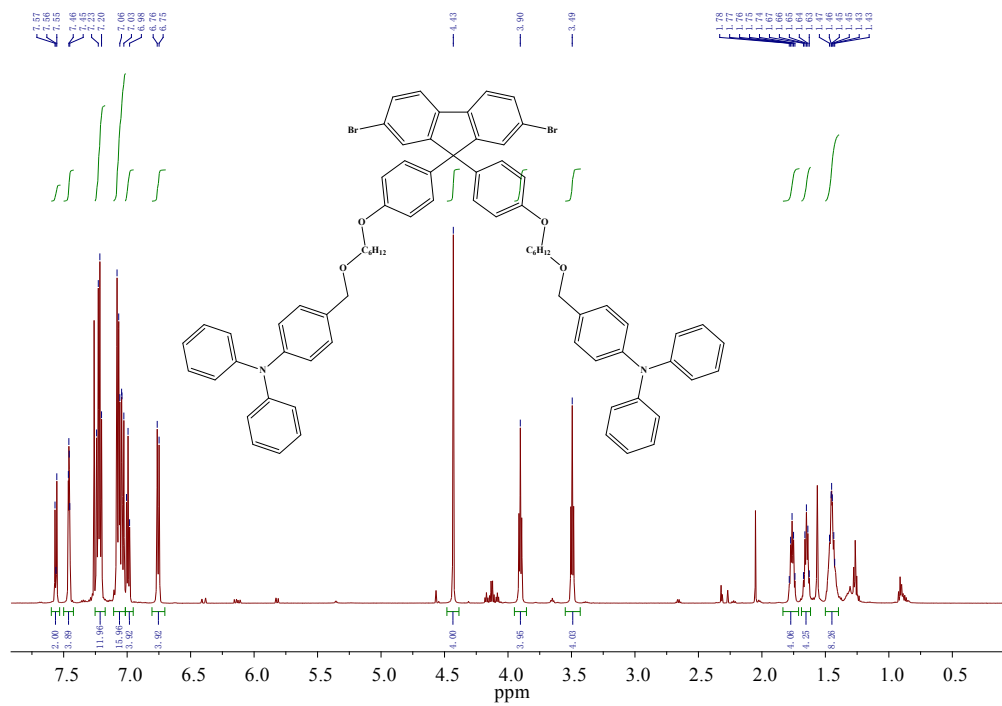


Fig. S7 $^1\text{H-NMR}$ of M2.

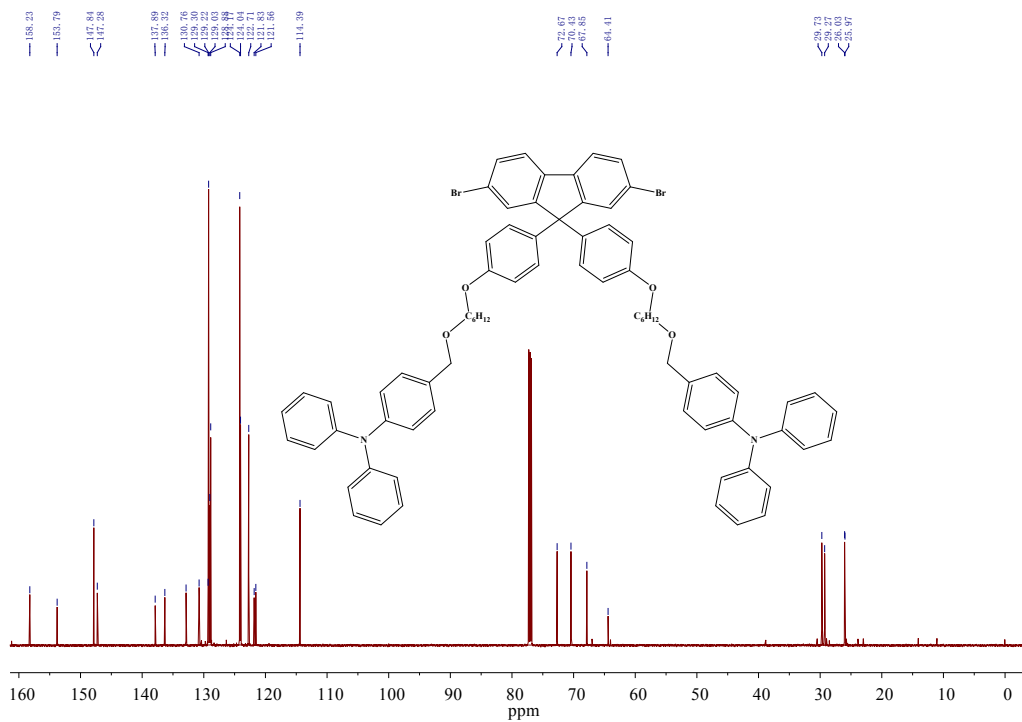


Fig. S8 $^{13}\text{C-NMR}$ of M2.

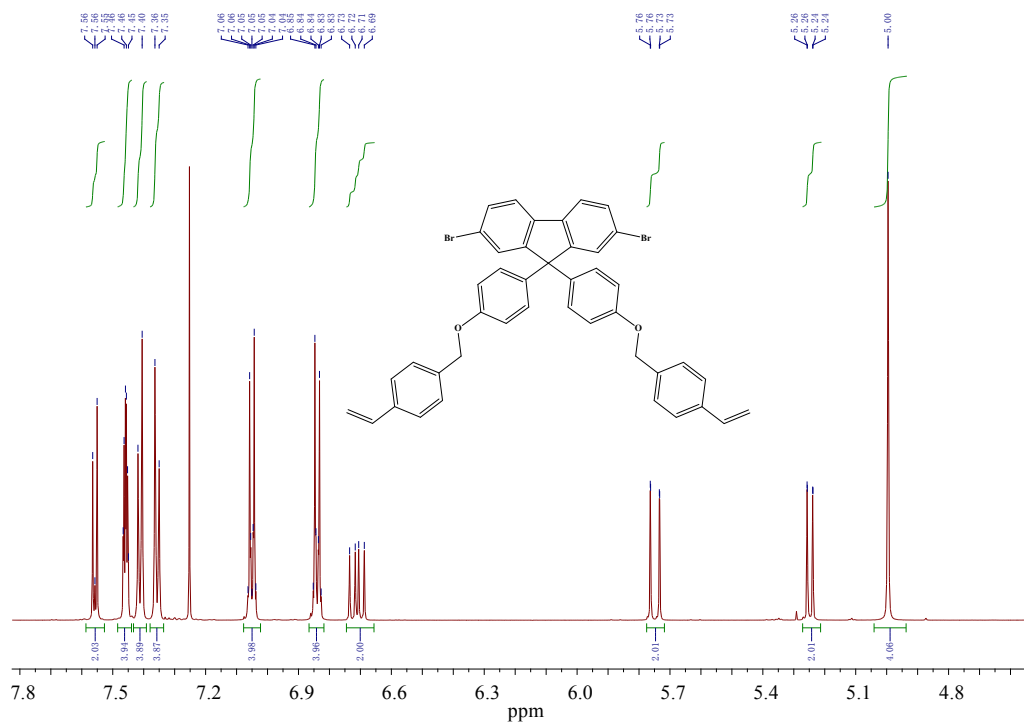


Fig. S9 ¹H-NMR of M3.

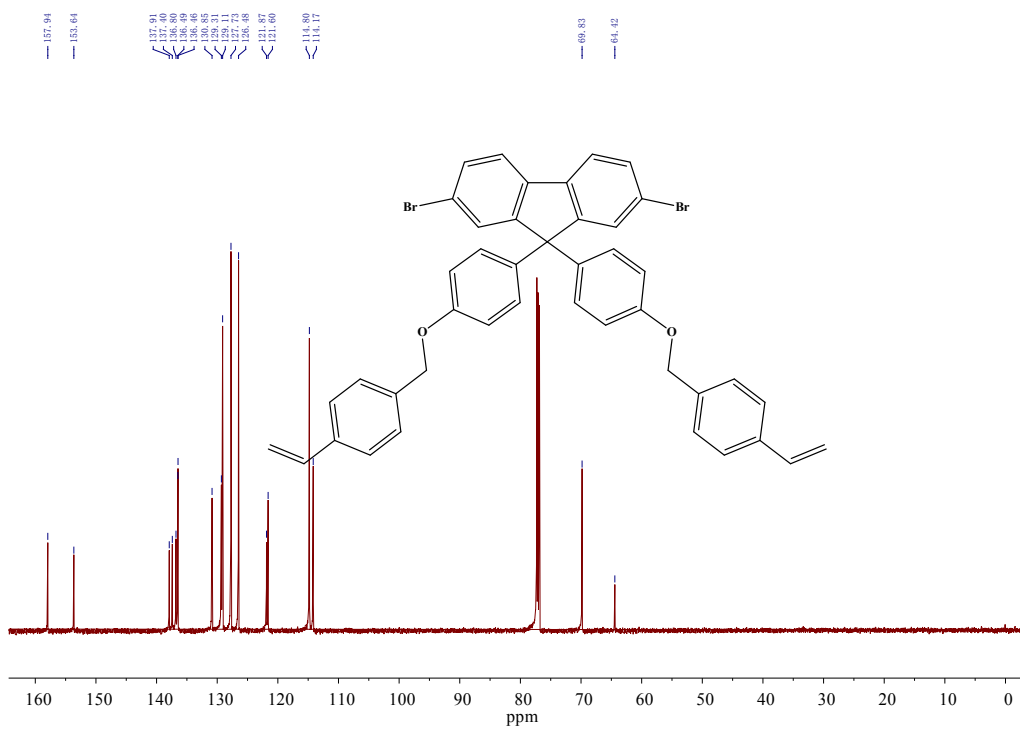


Fig. S10 ¹³C-NMR of M3.

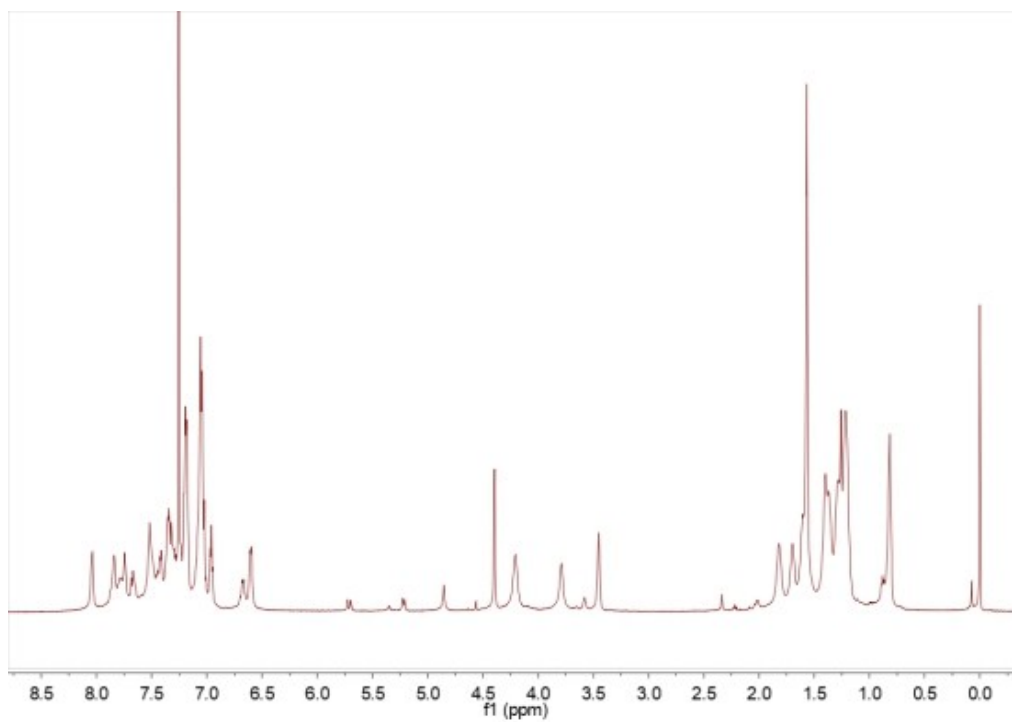


Fig. S11 $^1\text{H-NMR}$ of PFCTV10.

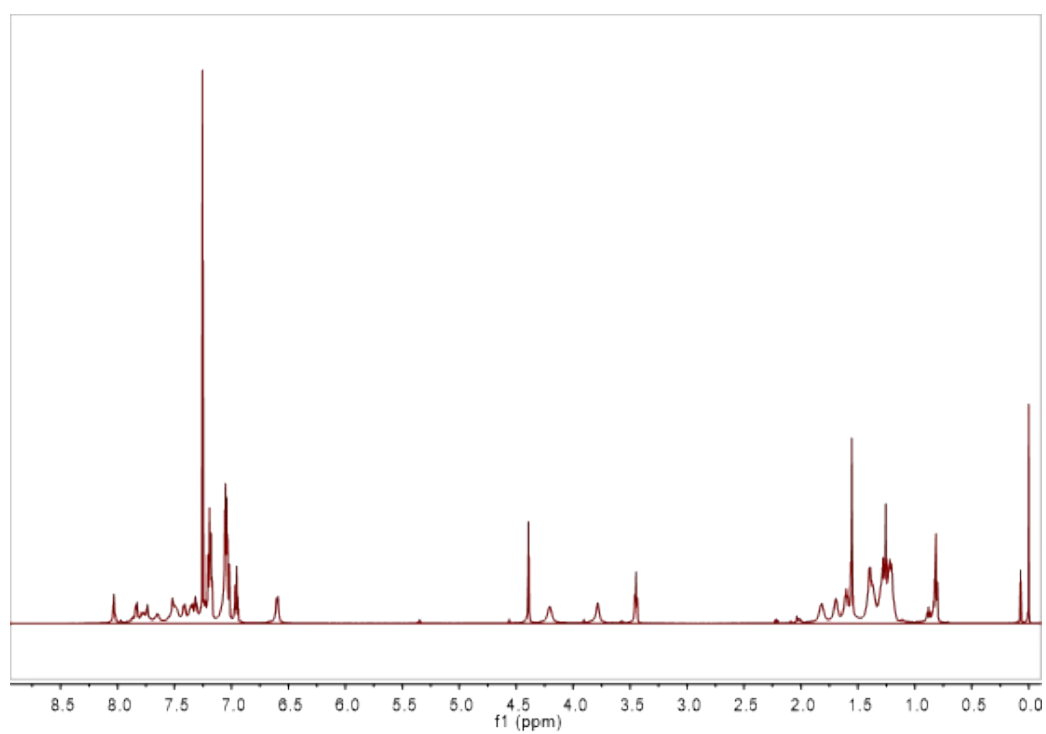


Fig. S12 $^1\text{H-NMR}$ of PFCT.

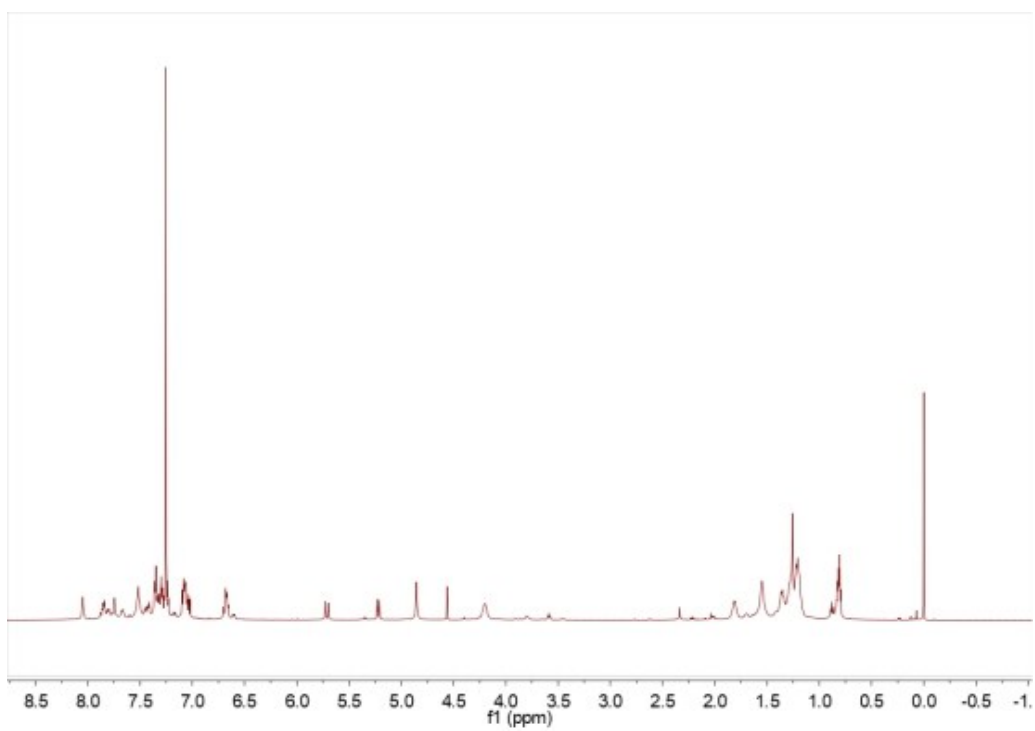


Fig. S13 $^1\text{H-NMR}$ of PFCTV20.

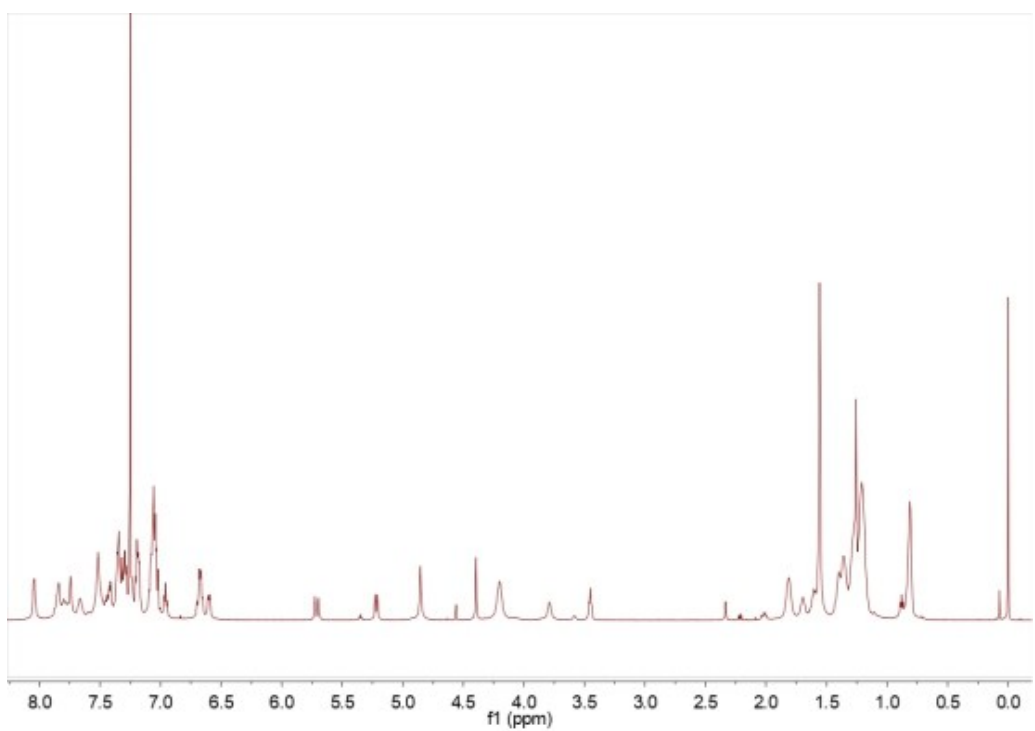


Fig.S14 $^1\text{H-NMR}$ of PFCTV30.

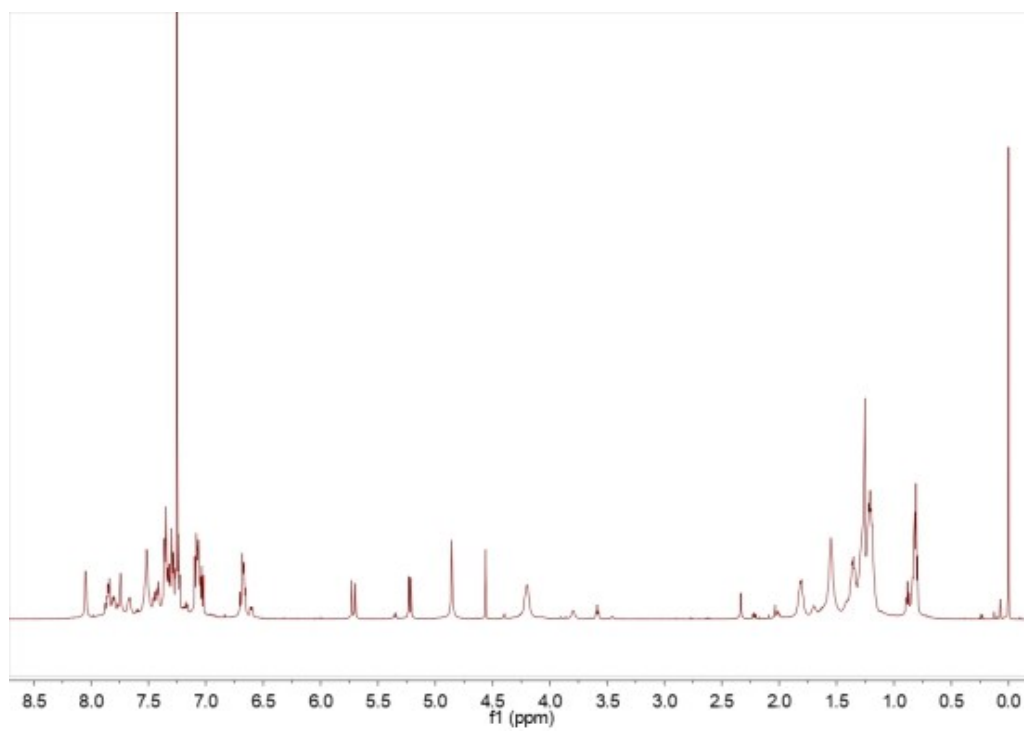


Fig. S15 ¹H-NMR of PFCTV40.